Broadband and omnidirectional antireflection from conductive indium-tin-oxide nanocolumns prepared by glancing-angle deposition with nitrogen

C. H. Chang, Peichen Yu,[a] and C. S. Yang
Department of Photonics and Institute of Electro-Optical Engineering, National Chiao Tung University, Hsinchu 30010, Taiwan

(Received 1 October 2008; accepted 11 January 2009; published online 6 February 2009)

Characteristic formation of highly oriented indium-tin-oxide (ITO) nanocolumns is demonstrated using electron-beam evaporation with an obliquely incident nitrogen flux. The nanocolumn material exhibits broadband and omnidirectional antireflective characteristics up to an incidence angle of 70° for the 350–900 nm wavelength range for both *s*- and *p*-polarizations. Calculations based on a rigorous coupled-wave analysis indicate that the superior antireflection arises from the tapered column profiles which collectively function as a gradient-index layer. Since the nanocolumns have a preferential growth direction which follows the incident vapor flux, the azimuthal and polarization dependence of reflectivities are also investigated. The single ITO nanocolumn layer can function as antireflection contacts for light emitting diodes and solar cells. © *2009 American Institute of Physics*. [DOI: 10.1063/1.3079329]

The ability to suppress or alter the Fresnel reflection of a material over a broad range of wavelengths and incidence angles brings exciting possibilities for next-generation optoelectronics. Over the last few years, the advance in nanofabrication technology has enabled the engineering of materials with desired refractive indices by adjusting the air fraction of nanocomposite materials.[1] Gradient-index (GRIN) coatings using various nanoporous materials including indium-tin-oxide (ITO), titanium dioxide (TiO_2), and silicon dioxide (SiO_2) have also been demonstrated.[2–4] However, the antireflective properties of the GRIN coatings are still limited by the number of layers available and the control of refractive-index profiles. On the other hand, subwavelength structured (SWS) surfaces based on the zero-order grating effect offer an alternative solution to extremely low reflectances.[5–7] In this context, since light cannot resolve the nanoscale textures, it averages the optical properties of the texture profile and behaves as if entering an effective medium. With a continuously varying profile, the effective medium exhibits gradient optical properties.[8] The SWS surfaces have several advantages over the conventional dielectric coatings such as broad angular and spectral responses, polarization insensitivity, and reliability in harsh and abrasive environments.[9] However, in order to control texture profiles, the subwavelength sized features are often fabricated by etching techniques.[6,10,11] Despite the superior antireflective properties, the involved fabrication costs can be significant. The resulting surface states could also degrade the performance of active devices, restricting the applications of SWS surfaces in optoelectronics. In this work, we introduce a deposition technique to form SWS surfaces using uniformly oriented ITO nanocolumns. The characteristic column formation is assisted by glancing-angle electron-beam deposition with an incident nitrogen (N_2) flux. The nanostructured material exhibits broadband and omnidirectional antireflective characteristics, which arise from the tapered column profiles. Since ITO has been widely used as a transparent conductive thin film in a variety of applications including organic and semiconductor light emitting diodes,[12] flat panel displays,[13] and solar cells,[14] the conductive ITO nanocolumns prepared by glancing-angle deposition are fully compatible with current technologies, offering a viable solution to boosting efficiencies of light emitting diodes and solar cells.[15]

Glancing-angle deposition is a physical deposition technique under conditions of obliquely incident vapor flux and limited adatom diffusion. The technique results in microscale and nanoscale porous thin films with oriented columnar structures toward the vapor source, owing to the nucleation formation and self-shadowing effect.[16] As shown in Fig. 1(a), a textured ITO thin film grown with an obliquely incident oxygen (O_2) flux shows oriented and closely packed columnar structures with assorted dimensions due to the random formation of nucleation cores. While such nanostructured

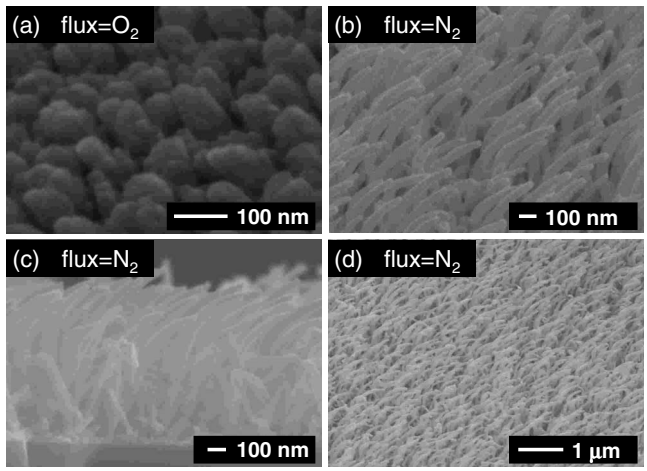

FIG. 1. SEMs for ITO nanocolumns deposited with an obliquely incident (a) oxygen flux and (b) nitrogen flux. The nitrogen assists in the characteristic column formation with tapered profiles. (c) The cross-sectional view of the oriented columns. (d) Tilted top view of the columns at a reduced magnification showing the uniform orientation and distribution.

[a]Electronic mail: yup@faculty.nctu.edu.tw.

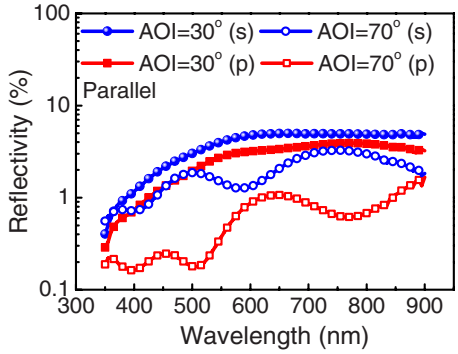

FIG. 2. (Color online) The measured reflection spectra of ITO nanocolumns shown in Figs. 1(b) and 1(c) at incidence angles of 30° and 70° are plotted for both polarizations in the 350–900 nm wavelength range. The plane of incidence is aligned to the orientation of nanocolumns.

material allows the refractive-index engineering, the profile is not suitable for SWS surfaces. Alternatively, we demonstrate the synthesis of ITO nanocolumns using glancing-angle deposition with a N_2 flux. As shown in Fig. 1(b), the ITO nanostructures deposited under the N_2 flow exhibit distinctive and uniformly oriented column profiles, following the direction of the incident vapor flux. The characteristic column formation presumably involves catalyst-free vapor-liquid-solid (VLS) growth, assisted by the introduced nitrogen. During the initial formation of nucleation cores, the nitrogen facilitates the segregation of tin-doped indium due to limited availability of oxygen atoms. The liquid-phase nucleation cores have a large accommodation coefficient which promotes the absorption of indium-oxide and tin-oxide vapors, leading to high growth rates.[17] Since surface diffusion determines the growth rate and the incident vapor flux determines the amount of atoms that could reach the surface, only those columns that interact with the vapor flux the most can continue the VLS growth, resulting in preferential column formation. Detailed formation mechanisms are discussed elsewhere.[18] As shown in Fig. 1(c), the columns are ~1.2 μm in length with a base diameter of ~100 nm and a top diameter of ~30 nm in diameter. The tapered column profiles, which are critical to the antireflective characteristics, resemble tilted cones with a density of $\sim 5 \times 10^9$ cm^{-2}. Figure 1(d) shows the scanning electron micrograph (SEM) of nanocolumns taken at a reduced magnification to demonstrate the uniformity. We are able to prepare a layer of uniformly distributed nanocolumns in single-step deposition up to an area of 2×3 cm^2. Ellipsometry measurements using *n* and *k* analyzers have also been performed for ITO nanostructures directly deposited on a silicon substrate. The nanostructured ITO layer deposited with O_2 shows thin-film-like reflectivity response, while the nanocolumns exhibit low reflectivities for the entire 350–900 nm wavelength range. Moreover, the resistivity of ITO nanocolumns is measured using a standard four-point measurement. It is believed that the incorporation of oxygen and oxygen vacancies is highly related to optical transmittance and resistivity of the ITO nanocolumns.[19] The sheet resistance can vary from tens to a few hundred ohms per square, depending on the nitrogen flow rate. Although for actual device applications a sheet resistance $<10\ \Omega$ per square is desired, the conductivities of ITO nanocolumns synthesized in a N_2 environment may be improved by a postannealing process with O_2.

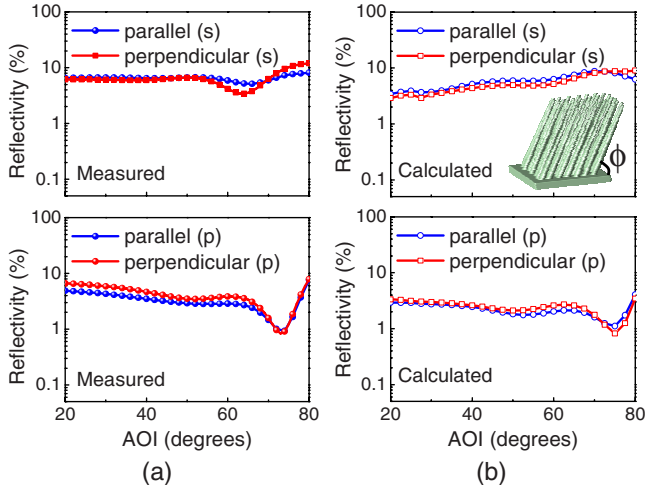

FIG. 3. (Color online) (a) The measured and (b) the calculated reflectivities of highly oriented ITO nanocolumns are plotted as a function of the incidence angle for both polarizations at the 632.8 nm wavelength. The characterizations and calculations are performed for the plane of incidence either parallel or perpendicular to the orientation of nanocolumns. The inset of (b) shows the simulated index profile of a unit cell consisting of 7×7 tilted random columns in an area of 1×1 μm^2.

To thoroughly investigate the antireflective characteristics of ITO nanocolumns, an angular reflection spectroscopy was performed for both *s*- and *p*-polarizations using an ellipsometer with a xenon lamp and a monochromator for wavelengths between 350 and 900 nm (V-VASE by J. A. Woollam Co., Inc.). Both the angle of incidence (AOI) θ_i and the angle of reflection θ_o were varied from 20° to 80°. The system was calibrated with a silicon substrate before each measurement. We also experimentally verified that the reflectivities contributed by high-order diffractions were negligible by fixing θ_i and scanning θ_o on the plane of incidence. The measured spectral reflectivities of ITO nanocolumns are shown in Fig. 2 for both AOI=30° and 70°, where the plane of incidence is aligned to the orientation of nanocolumns. As shown in Fig. 2, the reflectivities remain less than 6% for AOI up to 70° in the 350–900 nm wavelength range, covering the entire visible spectrum. The broadband antireflection properties are similar to those of GRIN coatings, in particular, the reduced reflection at short wavelengths. At large incidence angles, the nanostructured ITO behaves as an optically flat thin film, where the interference between the air/ITO and the ITO/Si interfaces can be observed. It is worth to note that since the interference is sensitive to the film thickness, slight nonuniformities in the nanocolumn density can manifest as large variations in reflectance measurements taken from different areas of a sample, which explains the discrepancy observed between Fig. 2 and Fig. 3(a) for *s*-polarization for an AOI of 70° at the 633 nm wavelength.

Next, the angle-dependent reflectivities for ITO nanocolumns were characterized at 632.8 nm wavelength for both *s*- and *p*-polarizations. The azimuthal dependence of reflectivities was also investigated with the plane of incidence either aligned or perpendicular to the orientation of nanocolumns. As shown in Fig. 3(a), the angular reflectivities of ITO nanocolumn structures are much smaller than those of a silicon substrate (~35% at normal incidence), showing excellent antireflective characteristics (<6%) up to incidence angles of 70° and 78° for *s*- and *p*-polarizations, respectively. Moreover, the measured reflectivities at the parallel and

TABLE I. The defined structural parameters of a unit cell consisting of 7×7 tilted random columns.

Structural parameters of nanocolumns	
Column density	4.9×10^9 cm^{-2}
Base diameter	100 nm
Top diameter	30 nm
Column length	1.2 μm
Tilt angle, ϕ	63.4°
Maximum position variation	36.25 nm

perpendicular azimuthal angles exhibit <2% variations for both polarizations.

We believe that the measured reflective characteristics of ITO nanocolumns result from the microscopic structures. Therefore, the reflectivities of ITO nanocolumns were theoretically investigated using an algorithm based on a rigorous coupled-wave analysis (RCWA). The RCWA method is often employed to solve for the diffraction and transmission efficiency of optical diffractive elements. The reflectivity is obtained as a sum of the reflection-diffraction efficiencies of different diffraction orders. A commercial implementation of the three-dimensional RCWA is employed in this study (DIFFRACTMOD, Rsoft Corporation).[20] The nanostructure consisting of 7×7 random columns is defined as a unit cell, where periodic boundary conditions are employed. The size of unit cell and randomness of nanopillar positions have been chosen to assure convergence. The structural parameters of nanocolumns, such as dimensions and densities, are extracted from the SEM graphs shown in Figs. 1(b) and 1(c) and are also summarized in Table I. Moreover, the material dispersion is taken into account by fitting the normally incident reflectivity spectrum of an ITO thin film deposited on a Si wafer. ITO becomes absorptive in the ultraviolet wavelength regime ($\lambda<400$ nm).[21,22] The angular and spectral reflectivities of ITO nanocolumns are then calculated using the extracted complex refractive indices. This approach has been applied to GaN nanorods and Si nanopyramids in the past.[23,24] The inset of Fig. 3(b) illustrates the simulated index profile of a unit cell, consisting of 7×7 tilted random pillars defined in an area of 1×1 μm^2. As also shown in Fig. 3(b), the calculated angular reflectivities of ITO nanocolumns agree reasonably well with the measurement for both polarizations and both azimuthal angles. In particular, the calculations correctly estimate the relative magnitudes in reflectivities for the planes of incidence with respect to angle and the AOI at which minimal reflectivities occur for *p*-polarization. We also find the specular reflection, i.e., the zeroth-order diffraction is indeed dominant in calculations, as being verified in the measurement, validating the RCWA method for modeling nanocolumns. Calculations indicate that the tapered column profiles contribute to the antireflection by collectively functioning as a graded-index layer. A further reduction in reflectivities is therefore achievable via nanocolumns with a larger base diameter. Finally, Fig. 4 shows that the reflective characteristics of ITO nanocolumns are relatively insensitive to polarizations. The variations in reflectivities are less than 2% for polarization angles rotating between 0° and 90°, characterized at wavelengths of 450, 550, and 632.8 nm for both AOI=30° and 70°. The variations are attributed to the column orientations. Similar characteristics have also been verified in calculation.

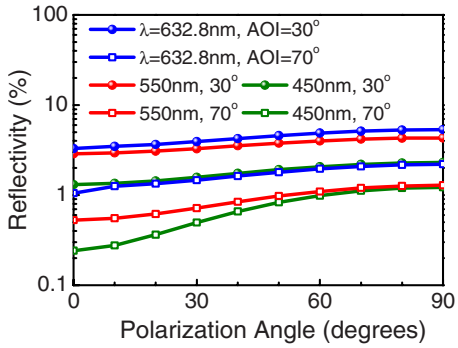

FIG. 4. (Color online) The reflectivities of ITO nanocolumns are characterized for polarization angles between 0° and 90° at wavelengths of 450, 550, and 632.8 nm for both AOI=30° and 70°. The reflective characteristics are relatively polarization independent, where the variations in reflectivities are less than 1%, possibly arising from the preferential column orientations.

The authors thank Dr. S. H. Hsu and Dr. Y. C. Chang at the Research Center for Applied Sciences, Academia Sinica in Taipei, Taiwan for the ellipsometry measurement. This work is supported by the National Science Council in Taiwan under Grant Nos. NSC 96-2221-E-009-092-MY3 and NSC 97-2120-M-006-009.

[1] D. E. Aspnes, Thin Solid Films **89**, 249 (1982).
[2] J. K. Kim, S. Chhajed, M. F. Schubert, E. F. Schubert, A. J. Fischer, M. H. Crawford, J. Cho, H. Kim, and C. Sone, Adv. Mater. (Weinheim, Ger.) **20**, 801 (2008).
[3] S. R. Kennedy and M. J. Brett, Appl. Opt. **42**, 4573 (2003).
[4] J. Q. Xi, M. F. Schubert, J. K. Kim, E. F. Schubert, M. Chen, S. Y. Lin, W. Liu, and J. A. Smart, Nat. Photonics **1**, 176 (2007).
[5] P. B. Clapham and M. C. Hutley, Nature (London) **244**, 281 (1973).
[6] Y. Kanamori, M. Sasaki, and K. Hane, Opt. Lett. **24**, 1422 (1999).
[7] P. Lalanne and G. M. Morris, Nanotechnology **8**, 53 (1997).
[8] D. H. Raguin and G. M. Morris, Appl. Opt. **32**, 2582 (1993).
[9] D. S. Hobbs, B. D. MacLeod, and J. R. Riccobono, Proc. SPIE **6545**, 65450Y (2007).
[10] Y. F. Huang, S. Chattopadhyay, Y. J. Jen, C. Y. Peng, T. A. Liu, Y. K. Hsu, C. L. Pan, H. C. Lo, C. H. Hsu, Y. H. Chang, C. S. Lee, K. H. Chen, and L. C. Chen, Nat. Nanotechnol. **2**, 770 (2007).
[11] M. E. Motamedi, W. H. Southwell, and W. J. Gunning, Appl. Opt. **31**, 4371 (1992).
[12] R. H. Horng, C. C. Yang, J. Y. Wu, S. H. Huang, C. E. Lee, and D. S. Wuu, Appl. Phys. Lett. **86**, 221101 (2005).
[13] B. H. Lee, I. G. Kim, S. W. Cho, and S. H. Lee, Thin Solid Films **302**, 25 (1997).
[14] H. Kobayashi, T. Ishida, Y. Nakato, and H. Tsubomura, J. Appl. Phys. **69**, 1736 (1991).
[15] C. H. Chang, P. Yu, C. H. Chiu, and H. C. Kuo, Proceedings of the 33rd IEEE Photovoltaic Specialists Conference, San Diego, CA, USA, 2008 (unpublished).
[16] M. M. Hawkeye and M. J. Brett, J. Vac. Sci. Technol. A **25**, 1317 (2007).
[17] S. Takaki, Y. Aoshima, and R. Satoh, Jpn. J. Appl. Phys., Part 1 **46**, 3537 (2007).
[18] P. Yu, C. H. Chang, M. S. Hsu, M. F. Su, and K. H. Wei (unpublished).
[19] G. B. González, T. O. Mason, J. P. Quintana, O. Warschkow, D. E. Ellis, J.-H. Hwang, J. P. Hodges, and J. D. Jorgensen, J. Appl. Phys. **96**, 3912 (2004).
[20] M. Nevière and E. Popov, *Light Propagation in Periodic Media* (Marcel Dekker, New York, 2003).
[21] N. Balasubramanian and A. Subrahrnanyarn, J. Phys. D **22**, 206 (1989).
[22] H. Kim, C. M. Gilmore, A. Piqué, J. S. Horwitz, H. Mattoussi, H. Murata, Z. H. Kafafi, and D. B. Chrisey, J. Appl. Phys. **86**, 6451 (1999).
[23] C. H. Chiu, P. Yu, H. C. Kuo, C. C. Chen, T. C. Lu, S. C. Wang, S. S. Hsu, Y. J. Cheng, and Y. C. Chang, Opt. Express **16**, 8748 (2008).
[24] C. C. Chen, P. Yu, and H. C. Kuo, Proceedings of the 2007 IEEE/LEOS International Conference on Optical MEMS and Nanophotonics, Hualien, Taiwan, 2007, pp.107–108.